

Dynamical suppression of sea level rise along the Pacific coast of North America: Indications for imminent acceleration

Peter D. Bromirski,¹ Arthur J. Miller,² Reinhard E. Flick,³ and Guillermo Auad^{2,4}

Received 22 October 2010; revised 22 March 2011; accepted 6 April 2011; published 8 July 2011.

[1] Long-term changes in global mean sea level (MSL) rise have important practical implications for shoreline and beach erosion, coastal wetlands inundation, storm surge flooding, and coastal development. Altimetry since 1993 indicates that global MSL rise has increased about 50% above the 20th century rise rate, from 2 to 3 mm yr⁻¹. At the same time, both tide gauge measurements and altimetry indicate virtually no increase along the Pacific coast of North America during the satellite epoch. Here we show that the dynamical steric response of North Pacific eastern boundary ocean circulation to a dramatic change in wind stress curl, τ_{xy} , which occurred after the mid-1970s regime shift, can account for the suppression of regional sea level rise along this coast since 1980. Alarmingly, mean τ_{xy} over the North Pacific recently reached levels not observed since before the mid-1970s regime shift. This change in wind stress patterns may be foreshadowing a Pacific Decadal Oscillation regime shift, causing an associated persistent change in basin-scale τ_{xy} that may result in a concomitant resumption of sea level rise along the U.S. West Coast to global or even higher rates.

Citation: Bromirski, P. D., A. J. Miller, R. E. Flick, and G. Auad (2011), Dynamical suppression of sea level rise along the Pacific coast of North America: Indications for imminent acceleration, *J. Geophys. Res.*, 116, C07005, doi:10.1029/2010JC006759.

1. Introduction

[2] Tide gauge estimates of sea level trends vary globally, depending on the ocean basin, local subsidence or uplift, and whether along eastern or western boundaries [Barnett, 1983]. Since the early 1990s, satellite altimeter measurements have provided global coverage of sea level height spatial variability as well as better estimates of global mean sea level (MSL) rise, confirming the basin dependence determined with tide gauges. Recently, much of the uncertainty [e.g., Barnett, 1984; Munk, 2002] associated with the magnitude and the underlying causes of the rate of global MSL rise has been resolved [e.g., Domingues *et al.*, 2008]. Numerous studies have investigated global MSL rise [e.g., Church and White, 2006; Douglas *et al.*, 2001], with estimates of global MSL rise of about 1–2 mm yr⁻¹ over the 20th century [Intergovernmental Panel on Climate Change, 2008]. Tide gauge records along the U.S. West Coast generally show consistent increasing trends over much of the

20th century (Figure 1) that are close to estimates of the rate of global MSL rise. Satellite altimetry indicates that global MSL rise has increased to about 3 mm yr⁻¹ since the early 1990s [Cazenave and Nerem, 2004], but trends along the west coast of North America estimated from tide gauge measurements, confirmed by satellite altimetry since 1992, indicate that coastal sea levels have remained approximately stationary since about 1980 (see Figures 1 and 2). Here we investigate the unexplained difference between global MSL and sea level rise along the U.S. West Coast.

[3] Increases and decreases in the North Pacific subtropical and subarctic (Alaskan) gyre circulation, such as those resulting from changes in forcing associated with the Pacific Decadal Oscillation (PDO) [Mantua *et al.*, 1997; Mantua and Hare, 2002; Cummins and Freeland, 2007], may account for a significant portion of both the interdecadal-scale modulation and decadal trends in regional or relative sea level (RSL) observed at coastal tide gauges along the North Pacific eastern boundary. In this study, RSL refers to regional fluctuations in sea level height (SLH) at interannual and longer time scales. Interdecadal fluctuations and longer trends in RSL in specific ocean basins are affected by thermocline depth changes associated with wind-forced changes in ocean circulation [Reid and Mantyla, 1976; Sturges and Hong, 1995]. In the North Pacific, Firing *et al.* [2004] showed that sea level at Hawaii is related to basin-scale sea level variability forced by wind stress curl and linked to Rossby wave thermocline fluctuations and circulation, but they did not address the important coastal variability that has the greatest societal impact.

¹Integrative Oceanography Division, Scripps Institution of Oceanography, University of California, San Diego, La Jolla, California, USA.

²CASPO Division, Scripps Institution of Oceanography, University of California, San Diego, La Jolla, California, USA.

³California Department of Boating and Waterways, Scripps Institution of Oceanography, University of California, San Diego, La Jolla, California, USA.

⁴Now at Bureau of Ocean Energy Management, Regulation and Enforcement, Herndon, Virginia, USA.

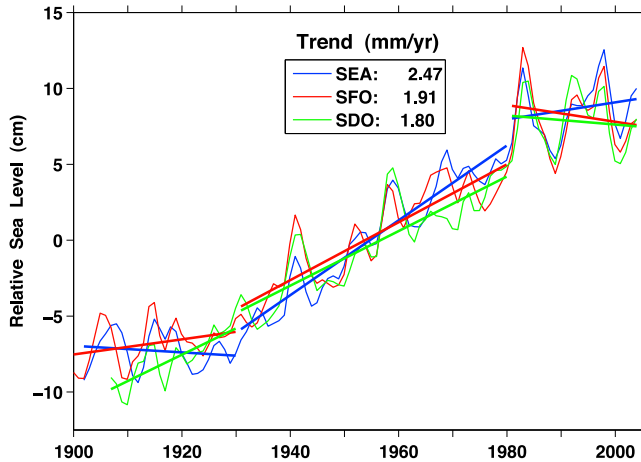


Figure 1. Decadal (low-pass-filtered) tide gauge SLH variability at the three stations with the longest records along the Pacific coast of North America at Seattle (SEA), San Francisco (SFO), and San Diego (SDO). The trends from 1930 to 1980 (box) are statistically significant from zero at the 97.5% level, while of the others, only the trend at SDO prior to 1930 is.

[4] The large-scale coherence of SLH on spatial scales on the order of 1000 km [Enfield and Allen, 1980; Chelton and Davis, 1982] suggests a regional influence on RSL at coastal locations. Estimates of local sea level rise at coastal tide gauge stations vary globally, so that local estimates of sea level change from tide gauge measurements of SLH over decadal periods refer to changes in RSL. Changes in RSL are reasonably well correlated on decadal time scales [Douglas et al., 2001]. RSL levels along the West Coast are strongly influenced by broad-scale ocean circulation patterns dynamically driven by surface winds [Reid and Mantyla, 1976] that may be associated with persistent climate regimes over the North Pacific basin.

[5] Because all potential driving forces that affect SLH are highly correlated, the statistical models used by Chelton and Davis [1982] were unable to determine whether residual SLH (with local atmospheric forcing removed) was dominated by basin-wide atmospheric forcing or from poleward propagating coastally trapped waves. Here we confirm the coastal SLH patterns determined by Chelton and Davis using a network of much longer tide gauge time series, augmented with spatial relationships using satellite altimetry SLH, ocean model hindcasts, and NCEP Reanalysis wind stress data [Kalnay et al., 1996].

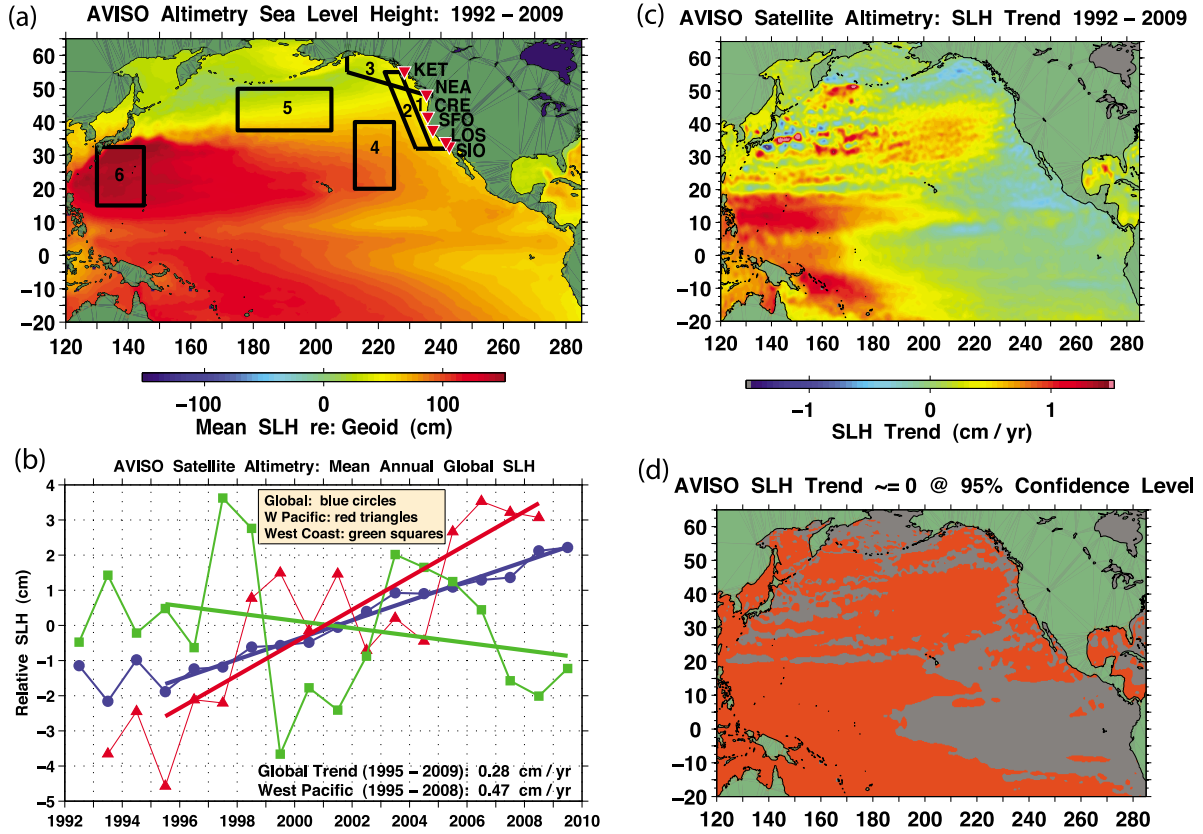


Figure 2. (a) Mean SLH across the North Pacific basin from 1992 to 2009, with locations of tide gauge stations used to determine coastal-to-basin-wide spatial relationships indicated. (b) Mean annual RSL curves across regions along the U.S. Pacific coast (region 1, green) and in the Western Pacific (region 6, red), compared with global MSL (blue). Regions 1–6 are referred to as R1–R6 in the text. Western Pacific and global upward trends in Figure 2b are statistically significant from zero at the 97.5 level, while the West Coast trend is not. (c) Least squares trends in SLH across the North Pacific basin, with (d) the T test trend analysis showing regions where the trend is significantly different from zero at the 95% level (red).

[6] The extent to which changes in RSL along the U.S. West Coast are affected by broad-scale climate patterns is important in planning and mitigating measures to preserve coastal assets that are vulnerable to elevated sea levels [e.g., *Heberger et al.*, 2009]. Rising RSL increases high tide water levels and allows more wave energy to reach farther shoreward, enhancing the potential for coastal flooding and associated impacts. Additionally, changes in associated upwelling and downwelling patterns can significantly affect coastal ecosystems, including fisheries [*Mantua et al.*, 1997].

[7] This paper is structured as follows. First we compare long tide gauge records, which first suggested recent suppression of sea level rise along the U.S. West Coast, with satellite altimetry data (Aviso, Ssalto/Duacs multimission altimeter products, 2010, <http://www.aviso.oceanobs.com/en/data/product-information/duacs/>, hereinafter Aviso2010). The satellite data allow linkage of coastal RSL variability measured by tide gauges with broad-scale SLH patterns across the North Pacific basin, as well as with other important oceanographic parameters such as sea surface temperature (SST) and surface winds. We next establish the relationship between these data and ocean model hindcasts over common record periods. We then explore the long-term spatial and temporal variability of SLH using a suite of ocean model simulations from 1948 to 2003 and NCEP Reanalysis wind stress data from 1948 forward [*Kalnay et al.*, 1996]. This enables inferences of the impact of climate-associated changes on coastal sea levels using ocean model thermocline depth estimates and wind stress curl data.

2. Tide Gauge and Satellite Altimetry Observations

[8] The longest tide gauge records along the U.S. West Coast were examined to compare trends and decadal variability (Figure 1). Points of inflection were chosen to reflect a change in the RSL trend that occurs near 1930 [*Douglas*, 1991] and the mid-1970s regime shift [*Miller et al.*, 1994]. Tectonic effects are likely strongest at Seattle (SEA), potentially affecting the trend estimates. The pronounced El Niño signal at all stations underscores the importance of the El Niño–Southern Oscillation (ENSO) for shelf processes along the West Coast. Interestingly southernmost San Diego (SDO) is not always dominant. Note that the difference between SDO and SEA was greatest prior to the inferred RSL rise acceleration after 1930 [*Douglas*, 1991] and the inferred deceleration after the regime shift. Although masked by the strong El Niño signals associated with the 1982–1983 and 1997–1998 El Niños, all three records suggest that the rate of RSL rise along the Pacific coast of North America decreased substantially since about 1980. The tide gauge data also suggest that a similar plateau in the rate of RSL rise occurred during the 1900–1930 epoch.

[9] The advent of satellite altimetry SLH measurements allows investigation of the relationship of sea level variability along the eastern boundary of the North Pacific basin with SLH variability across the basin, and associations with modes of climate variability. The broad-scale SLH variability was investigated using the merged, updated version of AVISO satellite altimetry data (Aviso2010). Mean RSL over the 1992–2009 satellite epoch shows that the greatest relative increase occurred in the Western Pacific (Figure 2,

R6). The rate of sea level rise varies appreciably over the basin (Figure 2c), with a near zero or decreasing trend along the Pacific coast of North America (Figure 2b; coastal R1 in Figure 2a). The R1 trend is consistent with that observed at tide gauges along the Pacific coast (Figure 1), which indicate that this trend extends backward to about 1980. In addition, the similarity of RSL variability over R2 (Figure 2b, dashed green), which extends R1 5° west, indicates that the eastern boundary RSL variability covers a relatively broad region and is not confined to the coast. The global trend of about 3 mm yr^{-1} (Figure 2b, blue curve) is consistent with that determined by *Cazenave and Nerem* [2004] and appears persistent. Note that coastal satellite SLH over R1 shows a pronounced El Niño signal, emphasized during the 1997–1998 El Niño, consistent with the tide gauge variability (Figure 1). Together, Figures 1 and 2 show that the coastal tide gauges and satellite altimetry have similar SLH variability and trends over their common record, and that both SLH measurements indicate that the recent rate of RSL rise along the Pacific coast is significantly lower than the global trend.

[10] The SLH patterns of variability across the Pacific are related to climate variability. Climate indices that are commonly used to describe the modes of climate variability across the North Pacific in addition to the PDO are the multivariate ENSO Index (MEI) [*Wolter and Timlin*, 1998], the North Pacific pattern (NPI) [*Trenberth and Hurrell*, 1994], and the Pacific North America pattern (PNA) [*Wallace and Gutzler*, 1981]. Correlation of these indices with altimetry SLH monthly anomalies gives similar PDO-like patterns of variability across the basin (Figure 3), with the region south of the Aleutians anticorrelated with coastal SLH. The MEI and PDO indices, which have strong month-to-month persistence due to the characteristics of the oceanic variables used to compute them, most strongly reflect the canonical pattern of oppositely signed correlations between the eastern and central North Pacific (Figures 3a and 3b). The meteorologically based indices (PNA and NPI) also reflect that pattern, but more weakly in their correlation maps (Figures 3c and 3d) because of weaker month-to-month atmospheric persistence. Monthly NPI, especially, has intense variability throughout the year that does not produce a strongly coherent broad-scale oceanic response in SLH. Annual mean NPI, in contrast, which emphasizes the more energetic winter (November–March) variations in atmospheric pressure, produces a stronger signature of the canonical North Pacific structure seen in Figures 3a and 3b and has been shown to be very highly correlated with the leading principal component of wind stress curl over the northeast Pacific [*Cummins and Lagerloef*, 2002] (see Table 1). Note that this canonical pattern is similar to that observed in the SLH trends across the basin (Figure 2c), indicative of a basin-wide response. Also note that sea levels are generally well correlated along the Pacific coast of North America and with SLH anomalies in the tropical Pacific, consistent with the strong El Niño association shown in Figure 1.

3. Comparison of Tide Gauge Observations With Ocean Model SLH Simulations

[11] Long-duration tide gauge records along the Pacific coast of North America were used to describe coastal SLH spatial variability. Tide gauge stations having records that

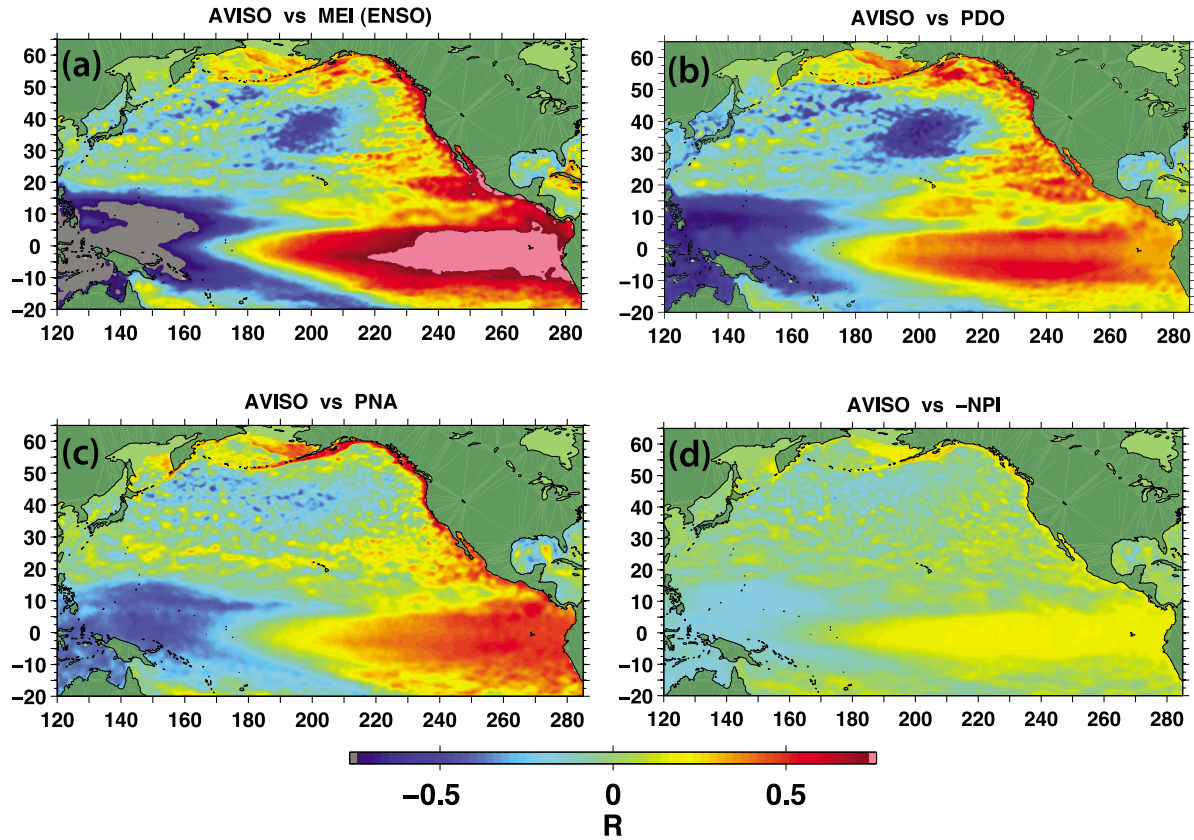


Figure 3. Correlations of satellite altimetry sea level height monthly anomalies 1992–2009 with (a) the multivariate ENSO index (MEI), (b) the Pacific decadal oscillation (PDO), (c) the Pacific-North America (PNA) index, and (d) the North Pacific index (NPI, 30°N–65°N to 160°E–220°E). Lower pressure over the region gives a more negative NPI, with the negative NPI correlated with SLH to give a pattern consistent with the other indices. The NPI is determined from sea level pressure anomalies over the central North Pacific, generating associated winds in that region. Thus the poorer correlation of remote SLP-associated NPI with coastal SLH is consistent with the dominant influence of relatively nearby τ_{xy} variability on sea level trends along the West Coast.

extend prior to 1948 at four California locations, La Jolla (SIO), Los Angeles (LOS), San Francisco (SFO), and Crescent City (CRE), and at more northern stations at Neah Bay, WA (NEA) and Ketchikan, AK (KET) were included in our comparisons (see Figure 2 for station locations). In addition, the station at Honolulu, HI (HON) was included to investigate the relationship between coastal and midbasin SLH variability. Anomalous data values resulting from either instrument malfunction or transposing errors were removed from the hourly data. The inverse barometer correction was

made using NCEP Reanalysis sea level pressure data [Kalnay *et al.*, 1996], and the seasonal cycle was removed for comparison with the ocean model data prior to forming monthly anomalies. For consistent comparisons, the seasonal cycle was also removed from the satellite altimetry and wind stress curl data, forming respective monthly anomalies.

[12] To estimate the significance of dynamical contributions to U.S. West Coast sea level trends, ocean hindcasts were analyzed for the time period 1948–2003 using Oberhuber's [1993] primitive equation isopycnal ocean model (OPYC)

Table 1. Correlation: West Coast Sea Levels and Wind Stress Curl With Climate Indices^a

	AVISO (1992–2010)		τ_{xy} (1948–2010)		Tide Gauge (1950–2004)	
	Mode 1 (49%)	Mode 2 (6%)	Mode 1 (51%)	Mode 2 (20%)	Mode 1 (60%)	Mode 2 (17%)
PDO	0.71	0.09	0.70	0.31	0.49	0.33
MEI	0.85	0.38	0.60	0.20	0.83	0.07
NPI	-0.63	0.08	-0.87	-0.28	-0.52	-0.22
PNA	0.82	0.14	0.90	0.30	0.63	0.30

^aCorrelation coefficients, r , between principal component modes 1 and 2 (percent variance explained in parentheses) of coastal winter (November–March) average anomalies over coastal region R1 (Figure 2) of altimetry SLH, wind stress curl (τ_{xy}), and West Coast tide gauge PC1 (see Figure 2 for station locations) and average winter PDO, MEI, NPI, and PNA indices of climate variability.

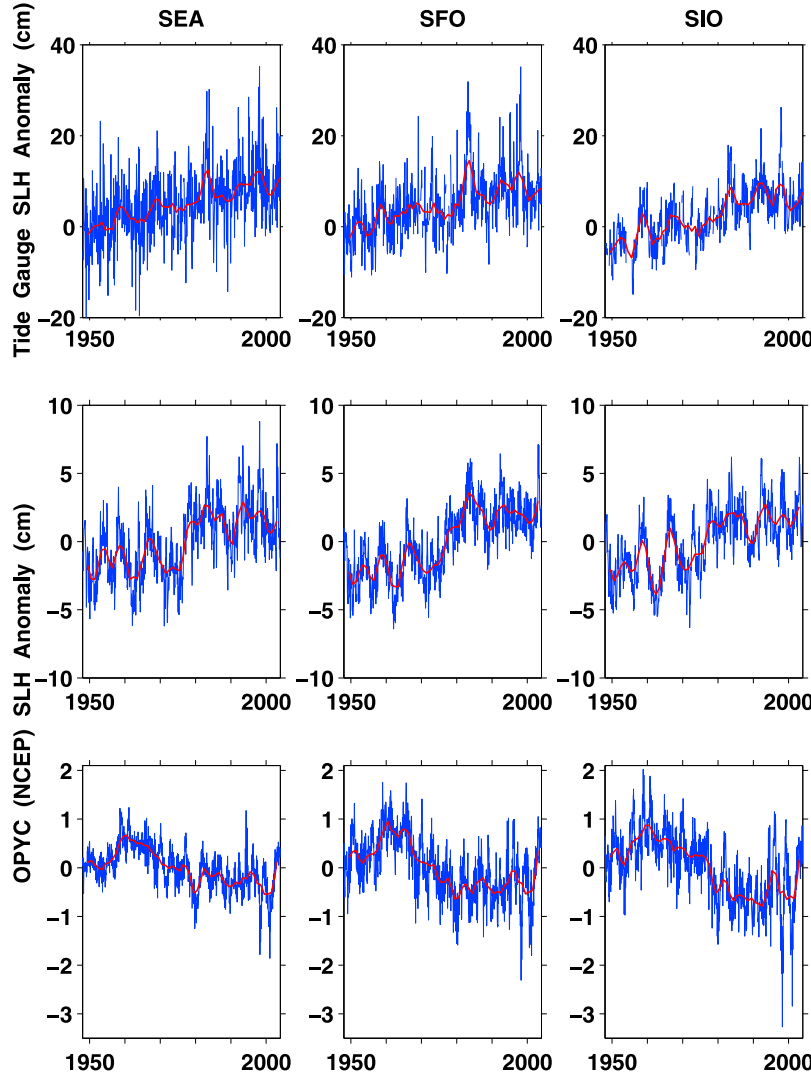


Figure 4. (top) Observed tide gauge sea level (sea level pressure corrected) monthly anomalies (long-term mean removed), with 3 year running means (red lines). The San Francisco (SFO) and La Jolla (SIO) regions are thought to be tectonically vertically stable, while the Seattle (SEA) region is probably not. (middle) Model sea level height bimonthly anomalies from the OPYC model hindcast forced with NCEP Reanalysis wind stress and heat flux anomalies. Note that the trends are weaker than the observed (i.e., Figure 4, top has *different scales*). (bottom) Model sea level height bimonthly anomalies from the OPYC ocean model hindcast forced *only* with NCEP heat flux anomalies. Note that the anomalies in this simulation are generally much smaller than forcing with both wind stresses and heat fluxes, indicating the dominance of wind stress forcing of RSL fluctuations.

forced by NCEP Reanalysis [Kalnay et al., 1996] wind stress and heat flux anomalies [Auad et al., 2001]. This model does not include eustatic or sea level pressure changes, so model SLH fluctuations are due solely to dynamical variability.

[13] Simulations using the primitive equation OPYC ocean model indicate that significant portions of observed variability and interdecadal changes in long-term trends in RSL along the U.S. West Coast can be explained by large-scale changes in North Pacific Ocean eastern boundary circulation driven primarily by atmospheric wind stress forcing (Figure 4, middle). Model results, however, reveal trends at coastal locations that are about half of the observed trends (compare Figure 4, top and Figure 4, middle). Additionally, the amplitudes of the modeled interdecadal RSL

variability using both wind stress and heat flux forcing are smaller than the observations by a factor of three. Yet modeled fluctuations correlate well with tide gauge observations (see section 4 and Figure 6), suggesting that estimates of the forcing magnitudes may be too small, that local topographic effects may be causing an enhancement of the observed coastal response, or that a remotely forced response may be important.

[14] The latter point was evident in that poleward propagating coastally trapped internal waves during the 1982–1983 and 1997–1998 El Niños are not as pronounced in the OPYC model hindcast animation as they are in the AVISO altimetry SLH animation during the 1997–1998 El Niño (not shown). Also note that interannual, decadal,

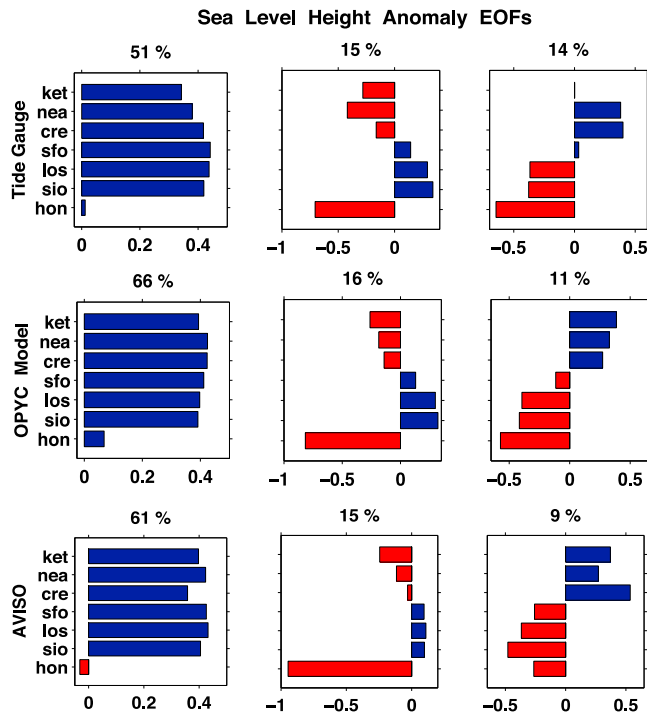


Figure 5. (top) EOF's of the first three modes of inverse barometer-corrected tide gauge SLH anomalies for 1948–2003 at stations (see Figure 2a for locations) KET (Ketchikan, Alaska), NEA (Neah Bay, Washington), CRE (Crescent City, California), SFO (San Francisco, California), LOS (Los Angeles, California), SIO (La Jolla, California), and HON (Honolulu, Hawaii). The observed patterns of variability are comparable to *Chelton and Davis* [1982], but here with longer records. The variance explained by each mode is indicated. (middle) OPYC model EOFs obtained for SLH anomalies over the 1948–2003 epoch at grid points approximately 1° west of the tide gauge station observations. (bottom) AVISO satellite altimetry EOFs obtained at grid points near those for the OPYC model over the 1992–2009 epoch. Note the strong similarity of the spatial patterns between the tide gauge, OPYC model, and satellite observations. Modes 1, 2, and 3 are shown from left to right for all data sets.

and multiyear El Niño Southern Oscillation (ENSO) variability obscures underlying long-term trends that are more evident in the longer tide gauge records (Figure 1). Because the ocean model underestimates SLH amplitudes, this also suggests that the higher amplitude fluctuations observed at coastal tide gauges may be enhanced by relatively local small-scale shelf dynamics not resolvable by the model (roughly 1.5° grid at these latitudes).

[15] To determine the relative importance of wind stress versus surface heat flux anomalies in driving RSL trends and interdecadal fluctuations along the North Pacific eastern boundary, we forced the ocean model with heat flux anomalies alone and compared it to the simulation forced with both wind stress and heat flux anomalies. Comparison of these simulations indicates that the fluctuations of SLH from the heat flux–only forced simulation are much smaller (by a factor of 5) than those of the complete-forced simulation

(Figure 4, bottom). This indicates that the wind stress forcing dominates the driving of interdecadal fluctuations of sea level in this region, and motivates our analysis wind stress curl variability below.

4. Large-Scale Spatial Patterns of Sea Level Variability

[16] Sea level along the West Coast is likely affected by broad-scale ocean circulation patterns that have resulted in the observed differential sea level rise (Figure 2). The SLH distribution is related to the dynamical steric response of the ocean to the combination of surface warming and changes in wind stress patterns, key factors that affect gyre circulation. The ocean's response to these forcings produces patterns in SLH that have associated patterns in SST. Two of these are commonly referred to as the PDO and the North Pacific Gyre Oscillation (NPGO) patterns (see Figure 3) [Mantua et al., 1997; Cummins et al., 2005; Di Lorenzo et al., 2008], which span the Pacific basin.

[17] Coastal RSL measured at tide gauges is likely to be correlated with large-scale patterns of sea level across the eastern North Pacific on interdecadal timescales [Qiu, 2002; Firing et al., 2004]. Yet it is unclear what fraction of the variance of observed local RSL at tide gauges is associated with these climate-forced large-scale patterns. This large-scale linkage was investigated in two ways. First, we computed EOFs of RSL from the SLP-corrected tide gauge data alone to determine alongshore coherency among the gauges. EOF mode 1 for the tide gauge observations (Figure 5, top) indicates that SLH at the coastal stations varies coherently, but that Honolulu (HON) sea levels explain little of the variance along the Pacific coast of North America. Mode 2 reveals an out-of-phase relationship between the coastal tide gauges north and south of 40°N (similar to the pattern observed by *Chelton and Davis* [1982]), again yielding no strong association with HON. The second EOF amounts to a mode that is dominated by mid-Pacific (HON) sea level with no significant response at the eastern boundary. The model EOF mode 1 (obtained at model grid points about 1° west of the tide gauge stations) has the same spatial structure and weightings as tide gauge mode 1 (Figure 5, middle), indicating that the OPYC model is capturing the dominant mode of coastal variability. The EOF patterns for altimetry SLH near the model grid points show a remarkably similar pattern, reinforcing the utility of using model output variability to investigate the ocean's dynamical response prior to the altimetry epoch.

[18] The large-scale relationship between coastal sea level in the model and open ocean sea level is illustrated with correlations between model hindcast SLH and altimetry SLH over the entire basin with the EOF mode 1 principal components (PC1) for tide gauge, nearby model SLH anomalies, and altimetry mode 1 over R1. These correlations (Figure 6) confirm that RSL along the North Pacific eastern boundary is coherent along the eastern boundary, but anticorrelated with sea level in the interior basin north of 20°N, reminiscent of the PDO pattern of SLH variability (see Figure 3). These results indicate the coastal mode of variability does not extend to Hawaii. In contrast, hydrographic analyses by Firing et al. [2004] show that HON SLH is highly correlated to open ocean sea level (dynamic height). How-

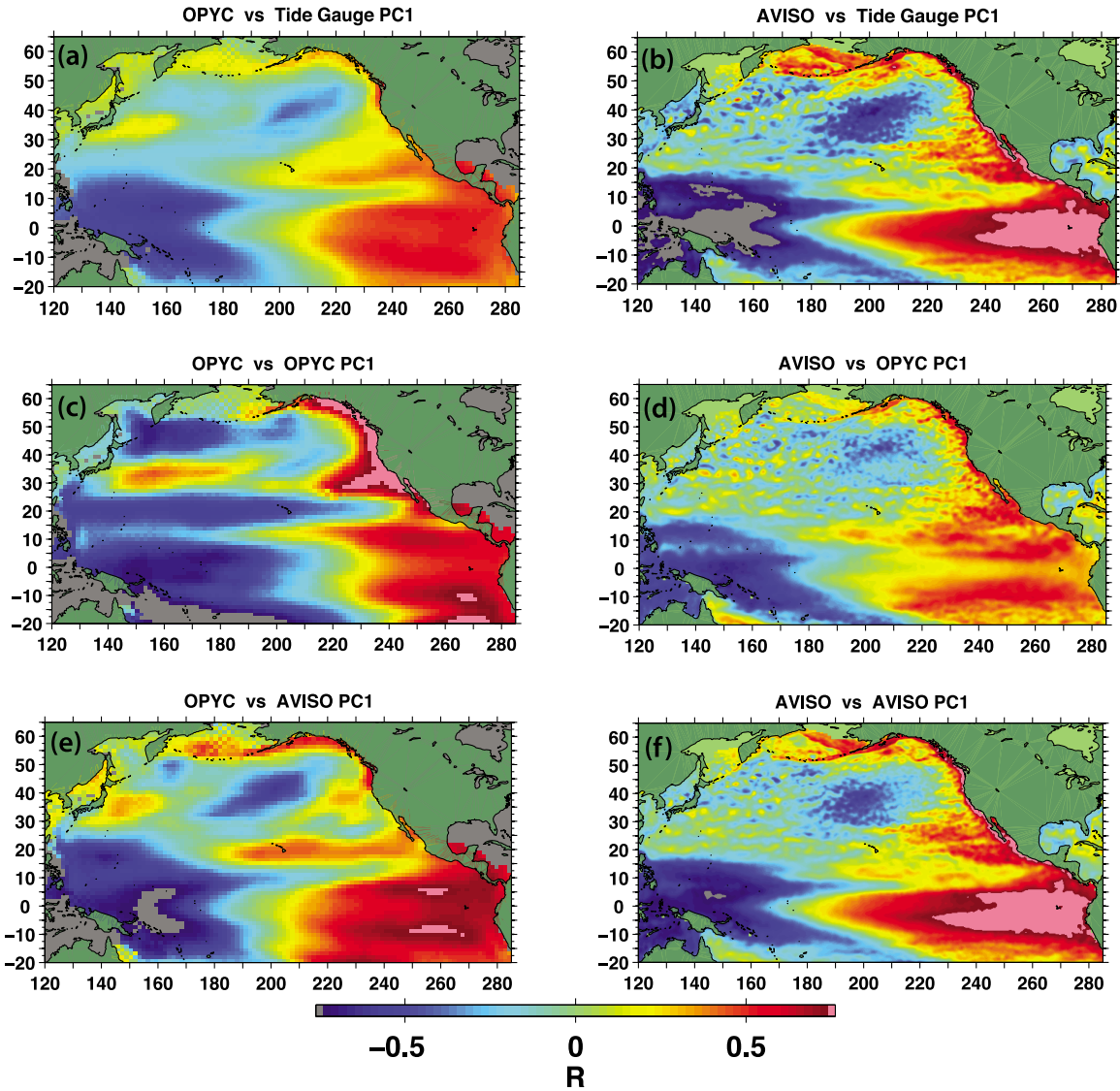


Figure 6. Correlation over 1992–2003 epoch between (a, c, e) ocean model SLH anomalies over the entire North Pacific basin and (b, d, f) AVISO altimetry SLH anomalies with EOF mode 1 principal components (PCs) of SLH anomalies of coastal tide gauges (Figures 6a and 6b), nearby ocean model (Figures 6c and 6d), and coastal R1 altimetry (Figures 6e and 6f). Note the generally weak correlation between eastern Pacific coastal sea level and Hawaii (202°E, 20°N).

ever, the patterns shown in Figures 2 and 6 indicate that that variability does not extend to the eastern boundary.

[19] Tide gauges along the coast and eastern boundary satellite altimetry measurements have similar associations with sea levels across the North Pacific basin. The similarity of the correlation patterns in Figure 6 reflects the relatively good correlation between SLH anomalies along the eastern boundary for both satellite and model SLH, and is consistent with their dominant mode 1 EOF spatial patterns (Figure 5 for 51%, 66%, and 61%). *Freeland* [2006] performed a similar EOF calculation but included several stations in the Gulf of Alaska and the Aleutian Islands. The structure of *Freeland*'s mode 1 EOF south of Ketchikan (KET) is consistent with our results. Reasons for the lack of correlation north of KET include contributions from the Aleutian stations, which are in

a region that does not exhibit the same characteristics as the other coastal stations in our study (see Figure 7a), and that near-coastal flows may affect the more northern Gulf of Alaska, non-Aleutian stations included by *Freeland*. Also in agreement with the EOF patterns in Figure 5 is the relatively poor correlation between coastal SLH and that observed at Hawaii (HON, Figure 6). Correlation between annual averages (June–May) of tide gauge PC1 and model SLH PC1 over coastal region R1 ($r = 0.49$, $p < 0.001$) confirms that the model captures much of coastal SLH variability.

5. North Pacific Wind Stress Curl Variability

[20] Both regional and remote gyre-scale circulation patterns likely contribute to sea level variability observed along

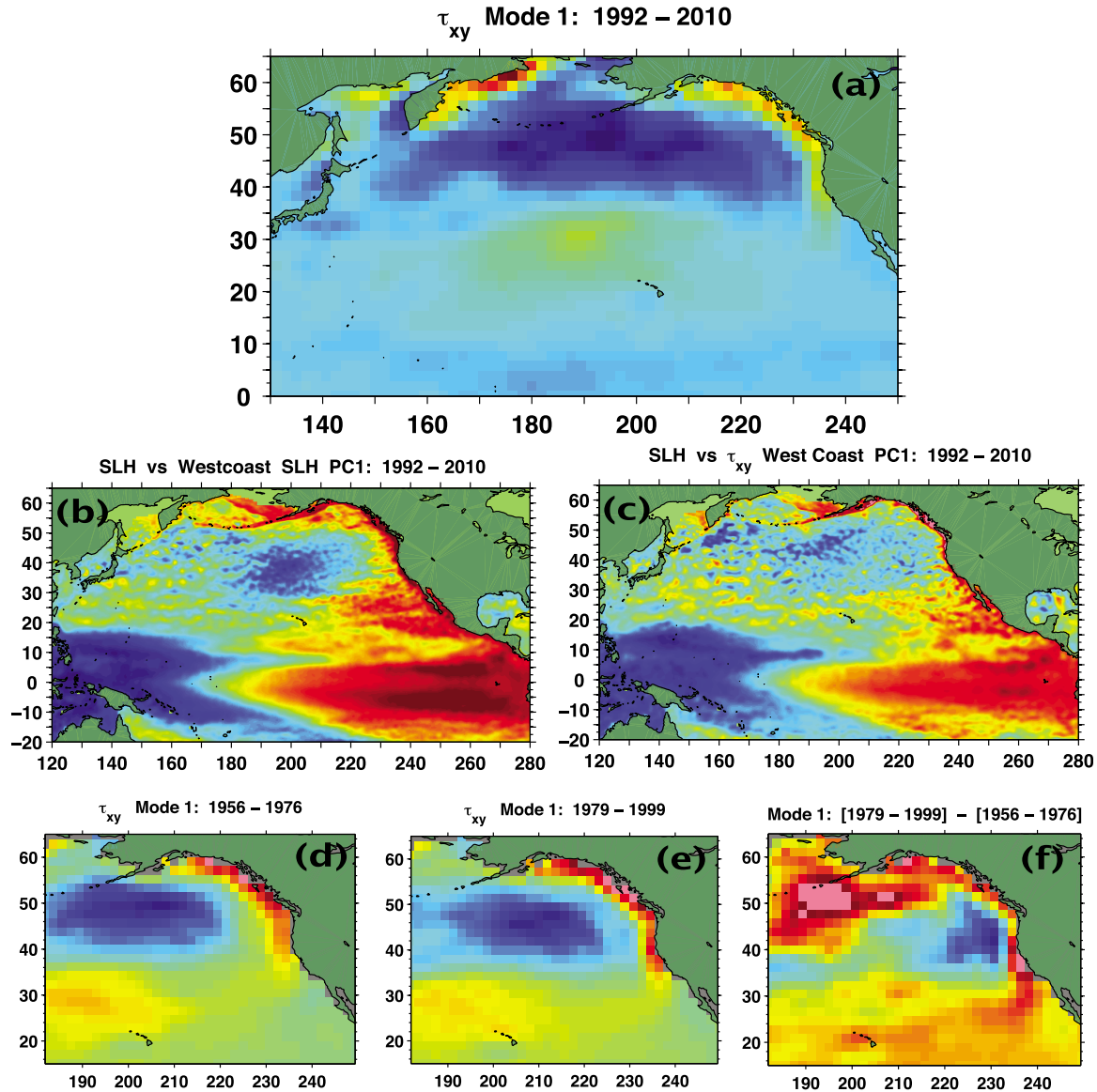


Figure 7. (a) Wind stress curl (τ_{xy}) monthly anomaly mode 1 variability across the North Pacific basin. Correlation maps of altimetry SLH over the basin with mode 1 principal components over coastal region R1 (see Figure 2) of altimetry (b) SLH and (c) τ_{xy} . The range of r values spans $[-0.75, 0.75]$ in Figure 7b and $[-0.5, 0.5]$ in Figure 7c. Wind stress curl monthly anomaly mode 1 patterns over the (d) 1956–1976 and (e) 1979–1999 epochs, with the (f) difference between the two epochs scaled to emphasize the change. Figures 7d and 7e have the same scaling as Figure 7a. Units are arbitrary.

the eastern boundary of the North Pacific. Persistent wind patterns associated with climate regimes have been shown to strongly influence sea level variability and trends in the southern Indo-Pacific region [Timmermann *et al.*, 2010]. Similarly, wind stress forcing must play a dominant role in determining the dynamical steric response in the eastern North Pacific, shown to affect North Pacific thermocline variability on interannual time scales associated with ENSO [Miller *et al.*, 1997]. As shown above (Figure 4), the OPYC ocean model simulations indicate that persistent wind stress patterns are the dominant factor affecting sea levels along the Pacific coast of North America. Consequently, the relationship between spatial changes in wind forcing and coastal sea level variability was investigated using monthly wind

stress curl (τ_{xy}) anomalies over the North Pacific determined from NCEP Reanalysis wind stress data [Kalnay *et al.*, 1996].

[21] The spatial pattern of the leading EOF mode of τ_{xy} over the North Pacific (Figure 7a, explaining about 10% of the variance) spanning the altimetry epoch has a relatively strong positive weighting over the eastern boundary of the North Pacific. Correlation of the leading principal components of both satellite SLH and τ_{xy} over coastal region R1 (see Figure 2) with satellite SLH across the basin show a similar pattern along the coast (Figures 7b and 7c), with an apparent strong association of coastal SLH with El Niño-induced tropical variability. These correlation maps have very similar PDO-like correlation patterns (see Figure 3), demonstrating the relationship of coastal RSL and τ_{xy} to

basin-wide SLH. Coastal altimetry SLH is well correlated with τ_{xy} over R1 (mode 1: $r = 0.65, p < 0.001$; mode 2: $r = -0.29, p = 0.007$) and also well correlated with tide gauge monthly anomalies (mode 1: $r = 0.49, p < 0.001$). The close association of coastal RSL and coastal τ_{xy} is further demonstrated by tide gauge PC1 being well correlated with PC1 of τ_{xy} over R1 ($r = 0.63, p < 0.001$) over the 1950–2004 time period. Thus, comparisons between the longer tide gauge, ocean model, and τ_{xy} time series allow investigation of historic RSL decadal variability and long-term trends not possible with the limited duration altimetry SLH currently available.

[22] Wind stress curl monthly anomaly mode 1 patterns over the 1956–1976 (Figure 7d) and 1979–1999 (Figure 7e) epochs show a shift in the dominant τ_{xy} pattern about 5° to the south and east. An intensification southward along the coast is highlighted by the difference between these EOF patterns that indicates a significant change in τ_{xy} along the coast (Figure 7f). This apparent shift is consistent with a change in wind patterns associated with the mid-1970s regime shift [Miller et al., 1994]. The first two leading principal components of τ_{xy} over coastal R1 are poorly correlated with an average of the West Coast upwelling index (UI) (Pacific Fisheries Environmental Laboratory, upwelling index, 2010, www.pfeg.noaa.gov/products/PFEL-modeled/indices/upwelling/NA/) from Pt. Conception to Vancouver. However, UI is significantly correlated with the third τ_{xy} mode that accounts for only 12% of the variance over R1 ($r = 0.28, p < 0.001$; 51% and 20% of the variance is accounted for by modes 1 and 2, respectively). This suggests that relatively small but persistent changes in wind stress over R1 can have a significant influence on coastal upwelling and affect coastal RSL and ecosystems.

[23] The association of τ_{xy} and SLH variability over coastal region R1 with broad-scale climate patterns was characterized by correlation of principal components of their first two modes of variability with the PDO, MEI, NPI, and PNA climate indices (Table 1). Because winter variability provides the greatest forcing for North Pacific Ocean circulation [Cayan, 1992], we compared winter (November–March) variability. All four indices have some association with R1 variability. The variance explained by each mode indicates the dominance of mode 1 for each coastal parameter. The high r values with low statistical significance for PC1 correlations indicate a high degree of variability, and suggests that multiple climate modes are concurrently affecting coastal sea levels, in agreement with the conclusions of Bond et al. [2003] for SST. These correlations show that, overall, the PNA is most closely associated with West Coast sea level variability, likely because the associated differential pressure systems that comprise the PNA have associated wind stress patterns that affect eastern boundary τ_{xy} . In contrast, the central Pacific NPI has the weakest overall association (see Figure 3), consistent with the inferred dominance of eastern boundary τ_{xy} affecting coastal sea levels.

[24] The relatively strong altimetry PC2 correlation with MEI indicates that regional altimetry most reliably captures the strong coastal SLH ENSO signature, particularly during the 1997–1998 El Niño. The significant impact of ENSO on coastal SLH (Figure 1) and the similarity of the patterns between coastal SLH and these indices with satellite

altimetry (compare Figures 3 and 6b) suggest that ENSO forcing may play a significant role in decadal-scale coastal SLH variability [Newman et al., 2003], in addition to the substantial interannual variability observed. Note that the longer τ_{xy} time series is significantly correlated with MEI for both PC1 and PC2, underscoring the importance of τ_{xy} on coastal sea levels and the strong association with ENSO shown in the correlation maps (Figures 3, 7b, and 7c).

6. Discussion

[25] Pronounced changes in several ocean parameters occurred around the time of the mid-1970s regime shift [Miller et al., 1994; Mantua et al., 1997]. Changes in the spatial patterns of τ_{xy} before and after the mid-1970s regime shift (Figures 7d, 7e, and 7f), together with τ_{xy} correlations with tide gauge and altimetry SLH data, suggest that the persistent atmospheric regimes that contribute to the PDO [Mantua et al., 1997] and the NPGO [Di Lorenzo et al., 2008] caused broad-scale changes in the North Pacific eastern boundary ocean circulation, affecting upwelling along the eastern boundary and suppressing the rate of RSL rise. Cummins et al. [2005] showed that SST and open ocean altimetry SLH are closely associated, having PDO spatial patterns that are similar to the correlation patterns of altimetry SLH and τ_{xy} (Figures 7b and 7c). These similarities are consistent with wind stress variability over the North Pacific providing the underlying forcing that produces these patterns.

[26] Average τ_{xy} (and thermocline) trends (Figure 8), obtained over coastal regions R1–R3 (Figure 2, roughly parallel to the coast), should be associated with broad-scale eastern boundary ocean dynamics. Positive (negative) τ_{xy} indicates upwelling (downwelling) conditions prevail. Upwelling tends to raise the thermocline and depress coastal sea levels. Downward (upward) trends in τ_{xy} are associated with upward (downward) trends in coastal RSL. Regionally averaged τ_{xy} along the eastern boundary shows that a dramatic change in τ_{xy} occurred during the mid-1970s (Figure 8a). This change from positive to negative (i.e., upwelling to downwelling conditions) would tend to deepen the thermocline and raise RSL.

[27] Although obscured by the strong 1982–1983 and 1997–1998 ENSOs, an apparent jump in observed coastal sea levels appears to have occurred post-1980 (Figure 1), consistent with coastal sea level changes expected during the PDO warm phase. The observed trends in SLH, in contrast, changed from rising to nearly stationary SLH at that time, which is not consistent with the expected SLH response to wind patterns associated with PDO-scale forcing. Apparently, the PDO regimes are associated with basin-scale τ_{xy} forcing patterns that result in a basin-wide effect that can be suppressed along the eastern boundary by the regional response to τ_{xy} . Regional wind patterns are apparently important when considering long-term eastern boundary SLH trends, as opposed to interannual to decadal-scale SLH variability where the canonical PDO pattern dominates.

[28] Model estimates of thermocline depth anomalies over R1 and R2 show that a significant change in its long-term trend occurred during the mid-1970s (Figure 8c). Note that estimates of anomalous thermocline variability over R1 and R2 are very similar, and consistent with the high correlation

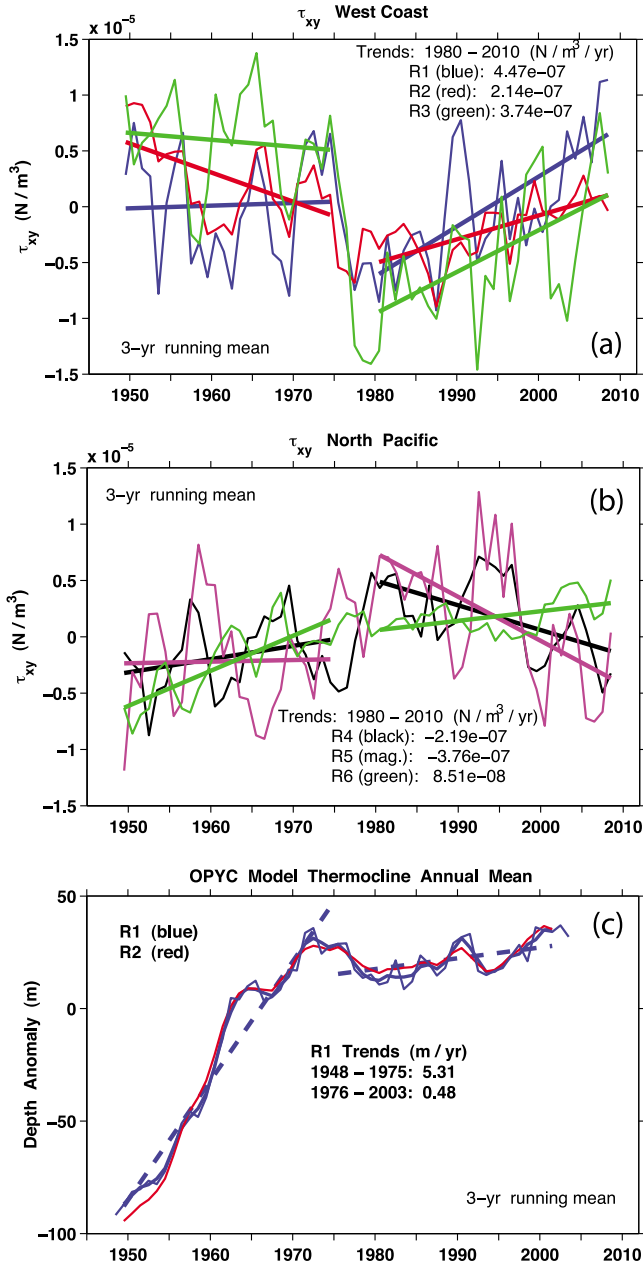


Figure 8. Mean wind stress curl, τ_{xy} , 3 year running means over (a) the eastern Pacific boundary regions R1, R2, and R3 (see Figure 2) and (b) noncoastal regions R4, R5, and R6. All trends after the mid-1970s regime shift are significant at the 97.5% confidence level or higher, while only those for R2 in Figure 8a and R6 in Figure 8b are. (c) Thermocline depth anomaly (thin blue) and 3 year running mean estimates (thick blue, red) from the OPYC model simulation forced with NCEP wind stress and heat flux anomalies over coastal regions R1 and R2. These model thermocline depth variability estimates were obtained by calculating the depth of the third isopycnal layer, which did not shoal, and correcting for the climatology at each grid point before obtaining the annual averages over each region. Trends (dashed lines, significant at the 97.5% level) show the dramatic change after the mid-1970s regime shift.

values of SLH and τ_{xy} extending westward from the coast (Figures 7b and 7c). The nearly constant long-term model thermocline anomaly levels post-1975 are consistent with nearly stationary RSL, and also consistent with altimetry and tide gauge measurements.

[29] The upward coastal τ_{xy} trends since 1980 (Figure 8a) indicate increasing upwelling [Schwing and Mendelsohn, 1997], which would suppress subsequent postregime shift RSL rise along the West Coast. The prior upward trend in coastal RSL from 1930 to 1980 (Figure 1) likely is more strongly associated with eustatic and other nondynamical thermally driven SLH changes in the North Pacific and the world's ocean, indicating the significance of global MSL trends. Large relatively short-term, primarily ENSO-associated τ_{xy} and RSL (Figure 1) fluctuations obscure long-term trends [Chambers et al., 2002]. However, the changes in τ_{xy} and RSL trends before and after the mid-1970s suggest persistent underlying wind stress regimes associated with decadal-scale climate variability. Alarmingly, τ_{xy} along the eastern boundary recently dropped to levels not observed since before the mid-1970s regime shift, when eastern boundary tide gauges recorded rising sea levels. This change in τ_{xy} may be foreshadowing a persistent shift to the PDO cold phase.

[30] Trends in τ_{xy} over noncoastal regions R4–R6 away from the eastern North Pacific boundary (Figure 8b) differ significantly from the R1–R3 trends, consistent with eastern North Pacific regional changes in wind stress being the dominant factor in suppressing sea level rise along the Pacific coast. However, basin-scale circulation patterns and broad-scale climate associations likely also influence eastern boundary sea levels [Latif and Barnett, 1994], as suggested by the correlations shown in Table 1. Their impact is apparent from the close associations of basin-wide τ_{xy} north of the equator (Figure 9a) and τ_{xy} over the PDO region (180° – 250° , 20°N – 62°N ; Figure 9b, red curve) with the PDO index (black curves), i.e., all show a change in phase during the mid-1970s. This is further supported by the similarity in correlation map patterns of the PDO and coastal SLH with basin-wide altimetry SLH (compare Figures 3b and 6b). However, annual mean τ_{xy} when averaged over the entire Pacific north of 20°N (Figure 9b, blue curve) has temporal variability that is distinctly different than when the tropics are included. This suggests that basin-scale forcing that includes the tropical Pacific (including atmospheric teleconnections [e.g., Alexander et al., 2002] and oceanic boundary-trapped waves with tropical origins [Pares-Sierra and O'Brien, 1989]), and not simply regional-scale τ_{xy} forcing, must be considered when attempting to explain regional sea level variability along the eastern boundary, because mass must be conserved when balancing the convergences and divergences induced by the Ekman pumping distribution. A full physics mass-conserving global ocean model is necessary to properly account for this effect. Similar to τ_{xy} over R1, τ_{xy} over the entire North Pacific basin (Figure 9a) has recently reached levels not seen since before the mid-1970s regime shift. Both regional and basin-wide wind stress measures suggest that a PDO regime shift may be imminent, with a concomitant change in τ_{xy} potentially resulting in a resumption of RSL rise along the Pacific coast of North America. Although previous studies

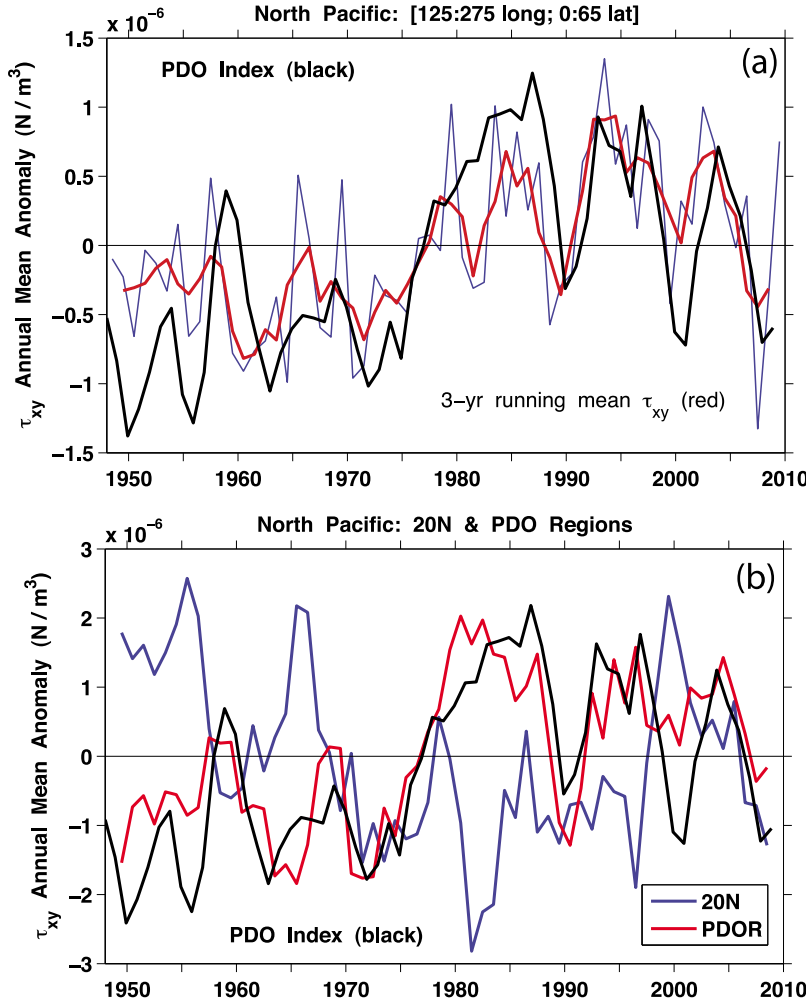


Figure 9. (a) Mean annual τ_{xy} over the North Pacific north of the equator (thin blue) and 3 year running means of τ_{xy} (red) and the scaled PDO Index (black). Correlation of the 3 year curves gives $r = 0.76$, $p < 0.001$. (b) The 3 year running means of mean annual τ_{xy} over the entire North Pacific north of 20°N, i.e., excluding the tropics, (blue), and over the PDO region (PDOR) east of the date line (red), with the scaled PDO index (black).

have suggested that a regime shift may have occurred following the strong 1999 La Niña [e.g., Peterson and Schwing, 2003], the subsequent oceanic conditions were not consistent with a regime shift. It is vital, however, to recognize that the recent τ_{xy} variability suggests the possibility of an impending regime shift, and if it occurs, the oceanic response may include the resumption of coastal RSL rise.

[31] The points of inflection in the tide gauge trends in Figure 1 were chosen based on results of previous studies, but they include some subjectivity. Other shorter epochs giving trend estimates less than the 20th century global MSL rise rate could have been selected. Elevated coastal SLH is associated with El Niño events. However, the mid-1970s change in τ_{xy} over the North Pacific (Figure 9a) tracks the decrease in SST over the basin [Latif and Barnett, 1996], consistent with a basin-scale response associated with the mid-1970s regime shift and the PDO shift from cold to warm phase. During the current PDO warm phase, coastal RSL has been stationary, while mean coastal RSL rose at about the global MSL rate during the preceding cold phase

from the mid-1940s to mid-1970s. This suggests an association of rising RSL along the Pacific coast of North America with the cold phase of the PDO.

7. Conclusion

[32] Tide gauge and satellite altimetry SLH measurements indicate that sea levels along the Pacific coast of North America have remained relatively stationary since about 1980, in contrast to the 3 mm yr^{-1} observed globally and about 6 mm yr^{-1} observed in the western Pacific. From about 1930–1980, RSL in this region rose at about the 2 mm yr^{-1} global MSL rise rate. A dramatic change in wind stress patterns occurred along the eastern boundary after the mid-1970s regime shift from cold to warm phases of the PDO, likely contributing to the change in the trend. Since roughly 1980, the predominant wind stress regime along the U.S. West Coast served to mitigate the rising trend in MSL, suppressing regional RSL rise below the global rate. Mean annual τ_{xy} over the entire North Pacific, associated with

decadal basin-wide ocean circulation oscillations that likely have a PDO connection, and over the eastern North Pacific have dropped to levels during 2008 not observed since before the mid-1970s regime shift. If this change in wind stress patterns persists, an associated regime shift to the PDO cold phase may result with a concomitant resumption of RSL rise along the West Coast approaching or exceeding the global MSL rise rate. A persistent change in eastern boundary τ_{xy} causing changes in upwelling/downwelling regimes and RSL rise along the West Coast would have important societal impacts, affecting coastal erosion and flooding, resources, and ecosystems.

[33] **Acknowledgments.** Support for this study from the California Department of Boating and Waterways, by NOAA through the ECPC (NA17RJ1231) and CPO (NA10OAR4310121), by NSF through OCE06-47815 and CCE-LTER OCE04-17616, and by the California Energy Commission through CIEE POCV02-S02, is gratefully acknowledged. Portions of this work were conducted in collaboration with SPAWAR Systems Center Pacific under grant SI-1703 from the Strategic Environmental Research and Development Program (SERDP). The AVISO altimeter products were produced by Ssalto/Duacs and distributed by AVISO, with support from CNES. Tide gauge data collected, archived, and distributed by the NOAA/NOS CO-OPS program are gratefully acknowledged.

References

- Alexander, M. A., I. Bladé, M. Newman, J. R. Lanzante, N.-C. Lau, and J. D. Scott (2002), The atmospheric bridge: The influence of ENSO teleconnections on air-sea interaction over the global oceans, *J. Clim.*, 15(16), 2205–2231, doi:10.1175/1520-0442(2002)015<2205:TABTIO>2.0.CO;2.
- Auad, G., A. J. Miller, J. O. Roads, and D. R. Cayan (2001), Pacific Ocean wind stresses and surface heat fluxes from the NCEP reanalysis and observations: Cross-statistics and ocean model responses, *J. Geophys. Res.*, 106(C10), 22,249–22,265, doi:10.1029/2000JC000264.
- Barnett, T. P. (1983), Recent changes in sea level and their possible causes, *Clim. Change*, 5(1), 15–38, doi:10.1007/BF02423425.
- Barnett, T. P. (1984), The estimation of “global” sea level change: A problem of uniqueness, *J. Geophys. Res.*, 89(C5), 7980–7988, doi:10.1029/JC089iC05p07980.
- Bond, N. A., J. E. Overland, M. Spillane, and P. Stabeno (2003), Recent shifts in the state of the North Pacific, *Geophys. Res. Lett.*, 30(23), 2183, doi:10.1029/2003GL018597.
- Cayan, D. R. (1992), Latent and sensible heat-flux anomalies over the northern oceans: The connection to monthly atmospheric circulation, *J. Clim.*, 5(4), 354–369, doi:10.1175/1520-0442(1992)005<0354:LASHFA>2.0.CO;2.
- Cazenave, A., and R. S. Nerem (2004), Present-day sea level change: Observations and causes, *Rev. Geophys.*, 42, RG3001, doi:10.1029/2003RG000139.
- Chambers, D. P., C. A. Mehlhaff, T. J. Urban, D. Fujii, and R. S. Nerem (2002), Low-frequency variations in global mean sea level: 1950–2000, *J. Geophys. Res.*, 107(C4), 3026, doi:10.1029/2001JC001089.
- Chelton, D. B., and R. E. Davis (1982), Monthly mean sea-level variability along the west coast of North America, *J. Phys. Oceanogr.*, 12(8), 757–784, doi:10.1175/1520-0485(1982)012<0757:MMSLVA>2.0.CO;2.
- Church, J. A., and N. J. White (2006), A 20th century acceleration in global sea-level rise, *Geophys. Res. Lett.*, 33, L01602, doi:10.1029/2005GL024826.
- Cummins, P. F., and H. J. Freeland (2007), Variability of the North Pacific current and its bifurcation, *Prog. Oceanogr.*, 75(2), 253–265, doi:10.1016/j.pocean.2007.08.006.
- Cummins, P. F., and G. S. E. Lagerloef (2002), Low-frequency pycnocline depth variability at Ocean Weather Station P in the northeast Pacific, *J. Phys. Oceanogr.*, 32(11), 3207–3215, doi:10.1175/1520-0485(2002)032<3207:LFPDVA>2.0.CO;2.
- Cummins, P. F., G. S. E. Lagerloef, and G. Mitchum (2005), A regional index of northeast Pacific variability based on satellite altimeter data, *Geophys. Res. Lett.*, 32, L17607, doi:10.1029/2005GL023642.
- Di Lorenzo, E., et al. (2008), North Pacific Gyre Oscillation links ocean climate and ecosystem change, *Geophys. Res. Lett.*, 35, L08607, doi:10.1029/2007GL032838.
- Domingues, C. M., J. A. Church, N. J. White, P. J. Gleckler, S. E. Wijffels, P. M. Barker, and J. R. Dunn (2008), Improved estimates of upper-ocean warming and multi-decadal sea level rise, *Nature*, 453, 1090–1093, doi:10.1038/nature07080.
- Douglas, B. C. (1991), Global sea level rise, *J. Geophys. Res.*, 96(C4), 6981–6992, doi:10.1029/91JC00064.
- Douglas, B. C., M. Kearney, and S. Leatherman (2001), *Sea Level Rise: History and Consequences*, Academic, San Diego, Calif.
- Enfield, D. B., and J. S. Allen (1980), On the structure and dynamics of monthly mean sea level anomalies along the Pacific coast of North and South America, *J. Phys. Oceanogr.*, 10(4), 557–578, doi:10.1175/1520-0485(1980)010<0557:OTSADO>2.0.CO;2.
- Firing, Y. L., M. A. Merrifield, T. A. Schroeder, and B. Qiu (2004), Interdecadal sea level fluctuations at Hawaii, *J. Phys. Oceanogr.*, 34(11), 2514–2524, doi:10.1175/JPO2636.1.
- Freeland, H. J. (2006), What proportion of the North Pacific current finds its way into the Gulf of Alaska?, *Atmos. Ocean*, 44(4), 321–330, doi:10.3137/ao.440401.
- Heberger, M., H. Cooley, P. Herrera, P. H. Gleik, and E. Moore (2009), The impacts of sea level rise on the California coast, *Rep. CEC-500-2009-024-F*, 101 pp., Calif. Energy Comm., Sacramento. [Available at http://www.pacinst.org/reports/sea_level_rise/report.pdf]
- Intergovernmental Panel on Climate Change (2008), *Climate Change 2007: Synthesis Report. Contribution of Working Groups I, II and III to the Fourth Assessment Report of the Intergovernmental Panel on Climate Change*, edited by Core Writing Team et al., 104 pp., Geneva, Switzerland.
- Kalnay, E., et al. (1996), The NCEP/NCAR 40-year reanalysis project, *Bull. Am. Meteorol. Soc.*, 77(3), 437–471, doi:10.1175/1520-0477(1996)077<0437:TNYRP>2.0.CO;2.
- Latif, M., and T. P. Barnett (1994), Causes of decadal climate variability over the North Pacific and North America, *Science*, 266(5185), 634–637, doi:10.1126/science.266.5185.634.
- Latif, M., and T. P. Barnett (1996), Decadal climate predictability over the North Pacific and North America: Dynamics and predictability, *J. Clim.*, 9(10), 2407–2423, doi:10.1175/1520-0442(1996)009<2407:DCVOTN>2.0.CO;2.
- Mantua, N. J., and S. R. Hare (2002), The Pacific Decadal Oscillation, *J. Oceanogr.*, 58(1), 35–44, doi:10.1023/A:1015820616384.
- Mantua, N. J., S. R. Hare, Y. Zhang, J. M. Wallace, and R. C. Francis (1997), A Pacific interdecadal climate oscillation with impact on salmon production, *Bull. Am. Meteorol. Soc.*, 78(6), 1069–1079, doi:10.1175/1520-0477(1997)078<1069:APICOW>2.0.CO;2.
- Miller, A. J., D. R. Cayan, T. P. Barnett, N. E. Graham, and J. M. Oberhuber (1994), The 1976–77 climate regime shift of the Pacific Ocean, *Oceanography*, 7, 21–26.
- Miller, A. J., W. B. White, and D. R. Cayan (1997), North Pacific thermocline variations on ENSO timescales, *J. Phys. Oceanogr.*, 27(9), 2023–2039, doi:10.1175/1520-0485(1997)027<2023:NPTVOE>2.0.CO;2.
- Munk, W. H. (2002), Twentieth century sea level: An enigma, *Proc. Natl. Acad. Sci. U. S. A.*, 99(10), 6550–6555, doi:10.1073/pnas.092704599.
- Newman, M., G. P. Compo, and M. A. Alexander (2003), ENSO-forced variability of the Pacific Decadal Oscillation, *J. Clim.*, 16(23), 3853–3857, doi:10.1175/1520-0442(2003)016<3853:EVOTPD>2.0.CO;2.
- Oberhuber, J. M. (1993), Simulation of the Atlantic circulation with a coupled sea ice-mixed layer-isopycnal general circulation model. Part 1: Model description, *J. Phys. Oceanogr.*, 23(5), 808–829, doi:10.1175/1520-0485(1993)023<0808:SOTACW>2.0.CO;2.
- Pares-Sierra, A., and J. J. O’Brien (1989), The seasonal and interannual variability of the California Current System: A numerical model, *J. Geophys. Res.*, 94(C3), 3159–3180, doi:10.1029/JC094iC03p03159.
- Peterson, W. T., and F. B. Schwing (2003), A new climate regime in northeast Pacific ecosystems, *Geophys. Res. Lett.*, 30(17), 1896, doi:10.1029/2003GL017528.
- Qiu, B. (2002), Large-scale variability in the midlatitude subtropical and subpolar North Pacific Ocean: Observations and causes, *J. Phys. Oceanogr.*, 32(1), 353–375, doi:10.1175/1520-0485(2002)032<0353:LSVITM>2.0.CO;2.
- Reid, J. L., and A. W. Mantyla (1976), The effect of the geostrophic flow upon coastal sea elevations in the northern North Pacific Ocean, *J. Geophys. Res.*, 81(18), 3100–3110, doi:10.1029/JC081i018p03100.
- Schwing, F. B., and R. Mendelsohn (1997), Increased coastal upwelling in the California Current System, *J. Geophys. Res.*, 102(C2), 3421–3438, doi:10.1029/96JC03591.
- Sturges, W., and B. G. Hong (1995), Wind forcing of the Atlantic thermocline along 32°N at low frequencies, *J. Phys. Oceanogr.*, 25(7), 1706–1715, doi:10.1175/1520-0485(1995)025<1706:WFOTAT>2.0.CO;2.
- Timmermann, A., S. McGregor, and F.-F. Jin (2010), Wind effects on past and future regional sea-level trends in the southern Indo-Pacific, *J. Clim.*, 23(16), 4429–4437, doi:10.1175/2010JCLI3519.1.

- Trenberth, K. E., and J. W. Hurrell (1994), Decadal atmosphere-ocean variations in the Pacific, *Clim. Dyn.*, 9(6), 303–319, doi:10.1007/BF00204745.
- Wallace, J. M., and D. S. Gutzler (1981), Teleconnections in the geopotential height field during the Northern Hemisphere winter, *Mon. Weather Rev.*, 109(4), 784–812, doi:10.1175/1520-0493(1981)109<0784:TITGHF>2.0.CO;2.
- Wolter, K., and M. S. Timlin (1998), Measuring the strength of ENSO events: How does 1997/98 rank?, *Weather*, 53, 315–324.

P. D. Bromirski, Integrative Oceanography Division, Scripps Institution of Oceanography, University of California, San Diego, La Jolla, CA 92093-0209, USA. (pbromirski@ucsd.edu)

R. E. Flick, California Department of Boating and Waterways, Scripps Institution of Oceanography, University of California, San Diego, La Jolla, CA 92093-0209, USA. (ref@coast.ucsd.edu)

A. J. Miller, CASPO Division, Scripps Institution of Oceanography, University of California, San Diego, La Jolla, CA 92093-0224, USA. (ajmiller@ucsd.edu)

G. Auad, Bureau of Ocean Energy Management, Regulation and Enforcement, 381 Elden St., Herndon, VA 20170, USA. (gauad@ucsd.edu)